Anthropogenic disturbances of natural ecohydrological processes in the Matlabas mountain mire, South Africa

AUTHORS:
Antoinette Bootsma[1]*
Samer Elshehawi[2,3]*
Ab Grootjans[2,4]
Piet-Louis Grundling[5,6]
Steven Khosa[7]
Mike Butler[8]
Leslie Brown[1]
Paul Schot[9]
*Joint lead authors

AFFILIATIONS:
[1]Department of Environmental Sciences, University of South Africa, Pretoria, South Africa
[2]Centre for Energy and Environmental Studies, University of Groningen, Groningen, the Netherlands
[3]Centre for Isotope Research, University of Groningen, Groningen, the Netherlands
[4]Institute of Water and Wetland Research, Radboud University Nijmegen, Nijmegen, the Netherlands
[5]Centre for Environmental Management, University of the Free State, Bloemfontein, South Africa
[6]Working for Wetlands, Natural Resource Management, Department of Environmental Affairs, Pretoria, South Africa
[7]South African National Parks, Pretoria, South Africa
[8]iThemba LABS – Environmental Isotope Laboratory, Johannesburg, South Africa
[9]Copernicus Institute of Sustainable Development, University of Utrecht, Utrecht, the Netherlands

CORRESPONDENCE TO:
Samer Elshehawi

EMAIL:
samer.shehawi@gmail.com

DATES:
Received: 26 Sep. 2018
Revised: 26 Jan. 2019
Accepted: 05 Feb. 2019
Published: 29 May 2019

HOW TO CITE:
Bootsma A, Elshehawi S, Grootjans A, Grundling P-L, Khosa S, Butler M, et al. Anthropogenic disturbances of natural ecohydrological processes in the Matlabas mountain mire, South Africa. S Afr J Sci. 2019;115(5/6), Art. #5571, 9 pages. https://doi.org/10.17159/sajs.2019/5571

ARTICLE INCLUDES:
☒ Peer review
☒ Supplementary material

DATA AVAILABILITY:
☐ Open data set
☐ All data included
☒ On request from author(s)
☐ Not available
☐ Not applicable

Matlabas is a mountain mire in Marakele National Park, located within the headwaters of the Limpopo River in South Africa. This mire consists of a complex of valley-bottom and seepage wetlands with small elevated peat domes. The occurrence of one decaying peat dome, which has burnt, and desiccated wetland areas with terrestrial vegetation has raised concerns. The aim of this study was to understand the mire features and water flows in order to identify the potential drivers causing wetland degradation. Wells and piezometers were installed to monitor the hydraulic head and collect water samples for analysis of ion composition, ^{18}O and ^{2}H stable isotope content, and $\delta^{13}C$ and ^{14}C isotope content for radiocarbon dating. Moreover, peat temperature profiles were measured and peat deposits were also dated using radiocarbon. Results indicate that the Matlabas mire developed in the lowest central-east side of the valley by paludification at the onset of the Holocene. During the Mid-Holocene, peat development was extended laterally by autogenic and allogenic processes. Three types of water flows driving peat development were identified – sheet flow, phreatic groundwater flow and deep groundwater flow – two of which are surface or near surface flows. The recent occurrence of decaying peat domes and desiccated wetland areas is possibly related to loss of exfiltrating deep groundwater flows that have resulted from drainage by the head-cut channels in the mire and interception of near surface water flow by an access road, respectively. Interventions should be undertaken to prevent further degradation of the mire.

Significance:

- This study is the first, as far as we are aware, on the ecohydrology of an inland mountainous mire in southern Africa.
- The results highlight the importance of the current wetland management (including rehabilitation) initiatives in South Africa.
- The integrative ecohydrological methods can be applied in other headwater wetlands in southern Africa.

Introduction

Peatlands play a crucial role as carbon sinks in the regulation of atmospheric CO_2 concentrations, which in turn influence climate.[1] Peatlands also provide ecosystem services like carbon sequestration, water storage and nutrient cycling.[2] Over the past two centuries, the health of peatlands and their ecosystem functions have been affected by direct and indirect use of these systems, e.g. use of peat for fuel, agriculture and groundwater extraction for drinking water.[2,3] Hence, there is growing attention on the assessment, conservation and restoration of peatlands on a global scale.[4] Mires are peatlands that are still actively accumulating peat, and this process is controlled by climate, hydrology and vegetation.[2] While near-natural mires are still widespread in the northern hemisphere – such as in Canada, Russia, Siberia and Finland[5] – they are relatively scarce in the southern hemisphere[2]. Nevertheless, the southern hemisphere's peatlands play an important role in the global carbon cycle.[6]

Pristine peatlands are rare in South Africa.[7] The best examples of pristine peatlands here are found along the eastern coast and in the central mountain areas. Two-thirds of South African peatlands occur along the northeastern seaboard of the Indian Ocean, known as Maputaland, in KwaZulu-Natal Province.[7] Maputaland contains both the largest peatland, the Mkuze peatland complex at 8800 ha, and the oldest mire, Mfabeni at 48 000 years.[8-11] The Matlabas mire, however, is situated in Marakele National Park in Limpopo Province, and is part of the Central Highlands Peatland Eco-Region.[12] Matlabas is one of the largest and least impacted spring mires known to exist in South Africa. The mire falls within the reaches of the Limpopo River, which suffers events of severe drought.[13] While the mire is largely in a good state, some signs of erosion were observed during a wetland inventory project undertaken in the park in 2008.[14] These signs included head cuts and gully erosion. Previous land-use practices (cattle farming) and road construction (see results), which took place in the 1960s up to the early 1980s, may have affected the mire's natural processes.[15] However, it is not known whether this erosion is increasing or what has caused it. These head cuts and gully erosion are expected to further increase peat drainage in the future, which could result in the loss of large sections of the mire. In the present study, we aimed to determine how the Matlabas peatland developed over time in relation to the principal water flows and recent changes in land use, as this knowledge will serve as a strong basis for effective conservation and rehabilitation planning.

Study area

Figure 1 shows the location of the Matlabas mire in the Waterberg Mountains, within Marakele National Park (an area of approximately 290.5 km²). The altitude of the Matlabas mire is around 1200 m above sea level (a.m.s.l.), and it has a total surface area of 64 ha, only 14 ha of which have peat accumulation. It has been managed as a national park since 1988 but was only officially proclaimed a national park on 11 February 1994. Before 1988, the area was used for agriculture, with both farming of crops and cattle grazing.[15]

EDITORS:
Nicolas Beukes
Yali Woyessa

KEYWORDS:
ecohydrology; peatland hydrology; stable isotopes; radiocarbon dating

FUNDING:
Ecological Restoration Advice (the Netherlands); Water Research Commission (South Africa)

The mire can be divided into two sides: a western side (6 ha) and an eastern side (8 ha). The western side of the mire drains from west (from 1621 m a.m.s.l.) to east along a slope of 4%, while the eastern side of the mire drains primarily to the north (from 1614 m a.m.s.l.) along a slope of 5%.[16] Two seepage wetlands upslope of the mire were intersected in the late 1960s by a road that runs along the southern edge of the mire. The mire is located close to a watershed within a major east to west stretching valley.

Matlabas is underlain by sandstone bedrock of the Aasvoëlkop Formation, part of the Matlabas Subgroup in the Waterberg Supergroup (with shale and mudstone), and the Sandriviersberg Formation, part of the Kransberg Subgroup also in the Waterberg Supergroup.[17] The formations developed on the parent materials range from shallow to deep sandy soils on sandstone and clayey soils on diabase dykes and mudstone.[15] Wetlands in the Waterberg Mountains mainly occur in the valleys, and are arranged in a prominent kite-like pattern as a result of the diabase dykes intruding along faults striking west-northwest to east-southeast and northeast to southwest into the Waterberg Supergroup sandstones.[16]

Average daily ambient temperatures range between a high of 19.5 °C and a low of 5.1 °C, with the maximum daily temperature reaching 22.8 °C and minimum night temperature reaching -1.7 °C. The average annual ambient temperature was 17.6 °C during the period 2011–2013.[16] Average rainfall during the same period was around 1000–1200 mm/year, with an average daily rainfall of about 5.5 mm/day during the hot and wet season, which takes place from October to April.[16]

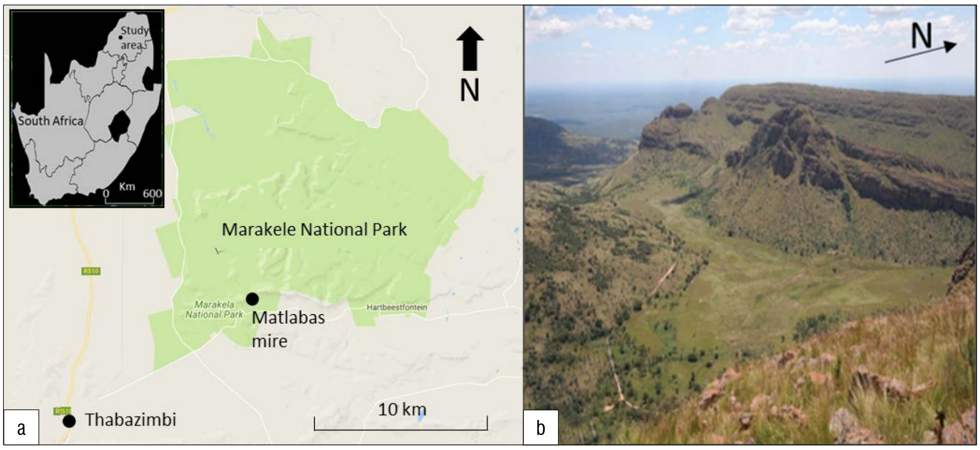

Figure 1: (a) Location of the Matlabas mire in Marakele National Park in South Africa (24°27'33.24"S, 27°36'1.28"E). (b) Overview of the Matlabas mire from a high plateau in the east.

Methods

Surface elevation and channel tracing

Elevations were determined with a differential GPS method, using a network of fixed, ground-based reference stations to broadcast the difference between the positions as indicated by the GPS and a known fixed position to obtain accurate contour lines at 50-cm intervals. Data for 290 points were obtained in February 2012 by F.J. Loock Surveyors Inc. from South Africa. The data were calibrated to height above sea level (a.m.s.l). Channelled surface water flows in the mire were recorded in the field by a hand-held GPS, visually plotted using aerial imagery and classified as either permanent or intermittent. Moreover, historical aerial images of the mire surface taken in 1956 and 1972, i.e. before and after road construction, were visually analysed.

Vegetation description

The different plant communities present in the area were mapped to determine their spatial spread as an indication of the inundation patterns. The Braun-Blanquet approach was followed to describe the vegetation.[18] Using aerial images, the area was divided into homogeneous units, in which a total of 54 sample plots (4x4 m) were placed in a randomly stratified manner per unit.[19] Plant species within the sample plots were identified and cover abundance values were assigned using the modified Braun-Blanquet scale.[20] Thereafter, a modified TWINSPAN was performed to classify the different plant communities present.[21] These vegetation patterns were used as environmental indicators to locate the zones of hydrological changes, and, therefore, to identify the most prominent sampling targets.

Peat thickness and dating

The thickness of the peat in the mire was recorded along four south-to-north running transects (A, B, C and D) covering the eastern side and at five points (W1 to W5) covering the western side (Figure 2). A Russian peat auger was used to sample peat cores, at 50-cm increments at a time, down to the top of the mineral soil.

A total of 14 peat samples (at a thickness of 1 cm) were collected for radiocarbon (^{14}C) dating to estimate the age at the bottom of the peat (at five locations) and to determine accumulation rates along two vertical profiles at points B3 (3 samples, a to c), B4 (6 samples, a to f) and C (2 samples, a and b). Samples from the vertical profiles were taken at the observed boundaries of facies change, e.g. degree of peat decomposition. Also, $\delta^{13}C$ content in the peat was measured to estimate the type of plant remnants forming the peat, i.e. C3, C4 or CAM (crassulacean acid metabolism) plants.[22] Each plant type has a different photosynthesis process, which leads to different $\delta^{13}C$

values as a result of the isotope fractionation.[23] C3 plants indicate wetter conditions with $\delta^{13}C$ values ranging from -22 to -25‰, and C4 plants indicate dry conditions with $\delta^{13}C$ values ranging from -11 to -14‰.[22,23] The colour and texture of each peat sample were described according to the Von Post Humification Scale,[24] and then the sample was sealed in a plastic bag. The samples were sent to the Centre for Isotope Research at the University of Groningen in the Netherlands for analysis.

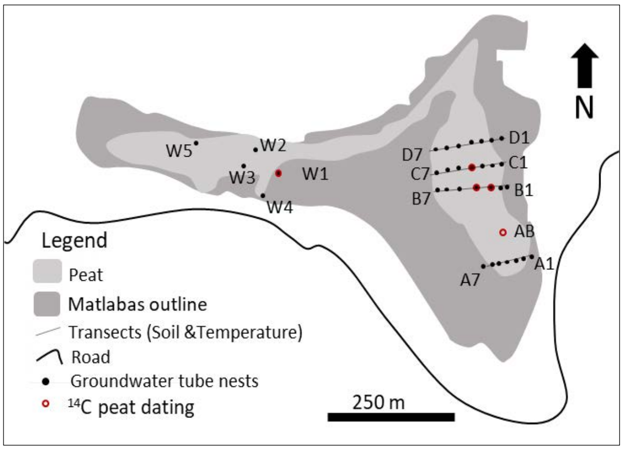

Figure 2: Location of sites used for soil description, radiocarbon peat sampling, groundwater wells for head measurement and groundwater samples for analysis of ion composition, stable isotopes and radiocarbon dating.

All the samples were treated using the acid-alkali-acid method to remove any contaminating material.[25] Then the $^{14}C/^{13}C$ content was measured by atomic mass spectrometry at the facility.[25] Most of the ^{14}C measurements were reported in before present (BP) units,[26] except for the samples with bomb effect backgrounds ($^{14}C>100\%$), while the $\delta^{13}C$ values were reported in permil (‰). The results in BP were calibrated to calendar age (CalBP) using the OxCal calculation model.[27] The calibration curve used for most of the samples was SHCAL13 for zone 1–2.[28] For the samples with ^{14}C content $>100\%$, the calibration curve accounting for the bomb effect was used.[29]

Groundwater flow

Phreatic and piezometric water levels

Polyvinyl chloride (PVC) groundwater tubes were installed to measure phreatic and piezometric water levels at various depths. Phreatic groundwater levels were measured using wells, with perforated screens placed along the entire tube, at a depth of 60–80 cm, in the peat layer. Piezometric water levels were measured using piezometers, with a 20-cm screen at the bottom of the tube placed in the underlying mineral soil. Observation nests, each consisting of one well and two piezometers, were installed at transects A, B, C and D on the east side and at points W1 to W5 on the west side (Figure 2). The 20-cm screens of the piezometer were inserted at two depths: the first was at a shallow depth of 60–80 cm in the peat layer (referred to as 'a' in the code) and the second in the mineral soil beneath the peat ('b'). Supplementary table 1 shows the depths of all the groundwater tubes. Water levels within the wells and piezometers were monitored manually on a monthly basis from 2011 to 2013 to obtain 24 months of consecutive readings.

Peat temperatures

Peat temperatures were measured to identify the direction of the groundwater flows in the peat layer.[30] They were measured using a 2-m-long steel probe along the four transects on the eastern side (A, B, C and D) at 20-cm depth intervals. The measurements were carried out at each transect during a cold and dry period in June 2011, with ambient air temperatures around 12 °C.

Ion composition

Water samples were collected from piezometers during a wet summer season in October 2011 and a dry winter season in June 2012, with 54 samples taken for each season. Another sampling round was added in October 2017, but there were only 29 samples because many piezometer tubes had been burnt by a natural fire. All piezometers were emptied with a hand pump one day before sampling to replenish the water before sampling. The sampled water was then stored in PVC bottles in volumes of 100 mL and 50 mL for cation and anion analyses, respectively, and kept in the dark at a temperature of 4 °C.

These water samples were analysed at the Agricultural Research Council laboratory in Pretoria, South Africa. The samples were passed over a 0.45-mu membrane vacuum filter to remove sediments and impurities. Water pH was measured by titration, and ion composition of Ca, Cl, NO_3, SO_4, PO_4, HCO_3, Mg, Na and K were measured by inductively coupled plasma mass spectrometry. In the third round of sampling, Fe and SiO_2 ions were also measured. The results were checked for deviations in ionic balance, and samples with deviations higher than 20–30% were disregarded in further analyses.

$^{18}O/^{2}H$ stable isotopes

In March 2014, 22 water samples were collected to measure the stable isotopes of oxygen and deuterium (^{18}O and ^{2}H) in the water (Figure 2, Supplementary table 2). These water samples were collected in dark glass bottles of 50 mL and 30 mL and stored in the dark at a temperature of 4 °C. Later, they were analysed at the Centre for Isotope Research laboratory by dual inlet isotope ratio mass spectrometry (DI-IRMS). The sampling was repeated in October 2017 (29 samples), and these samples were analysed at the Environmental Isotope Laboratory of iThemba LABS at the University of the Witwatersrand, South Africa. The stable isotope ratios in the samples ($\delta^{18}O$ and $\delta^{2}H$) were reported in ‰ w.r.t. VSMOW, i.e. the reference used was the Vienna convention material.[31]

Carbon isotopes

The radiocarbon content of water samples is an indication of the residence time of groundwater in the soil.[32] Six water samples were taken, using 500-mL dark glass bottles, from the piezometers in the sand layer at the end of the dry season in October 2017 to measure the radiocarbon content. Five points were selected on the eastern side at transects A, B and D (A2, B4, B6, D4 and D5) and one point on the western side of the mire at W5 (Figure 2). These samples were analysed for their carbon isotope content ($\delta^{13}C$ and ^{14}C) at the Centre for Isotope Research laboratory. $\delta^{13}C$ values of the samples were analysed using DI-IRMS and reported in ‰ w.r.t. VSMOW, similarly to the stable isotopes. The ratios were then used to infer whether there had been dilution of the ^{14}C values as a consequence of infiltration through the peat layer, which is indicated by $\delta^{13}C$ values lower than -16‰.[32]

Results

Elevation and peat thickness

The peat soils in Matlabas cover a total of 14 ha, which is only 22% of the larger wetland area of 64 ha. Peat depth varied from 30 cm at the steep slopes to almost 5 m in the central parts of the eastern side of the mire, while average peat thickness was 1.5 m. Hence, the estimated volume of the peat layer was around 150 000 m^3. Most of the peat layers were fibrous, and they were interrupted by clay and sand layers at the bottom, where some layers of gravel occurred, e.g. at B4.

Six channels with concentrated surface water flow were identified (Figure 3). Two of these are permanent water flow channels on the eastern side. A third channel starting from the western side also has a permanent flow. The permanent channels are incised about 40–50 cm into the peat. Surface water drains the mire in a northerly direction.

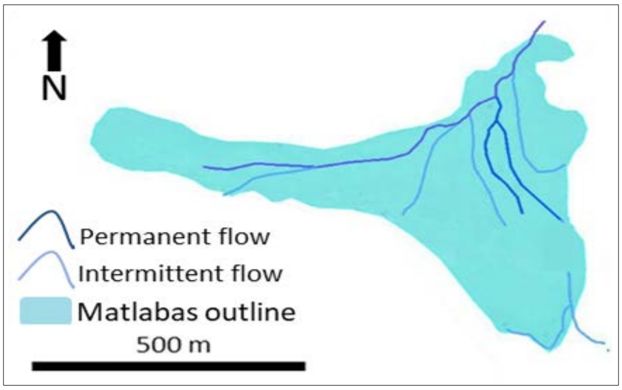

Figure 3: Map of water flow channels.

Aerial images taken in 1956 and 1972 show the mire before and after the road was built. These images show that some channel formation was already apparent in 1956 (Figure 4a). Since the construction of the road in the late 1960s, however, channel formation in the eastern section of the mire had increased in number and volume by 1972 (Figure 4b). Furthermore, the extent of two seepage wetlands visible on the 1956 images south of the later constructed road are largely reduced in the 1972 images.

Moreover, the mire has developed a series of elevated peat domes, with heights of approximately 1 m above the surrounding landscape and widths between 3 m and 9 m (Figure 5a). Most domes are situated along a fault line in a northwest-southeast direction, shown in a geological map of the area,[17] but some are also aligned in an east-west direction (Figure 5b).

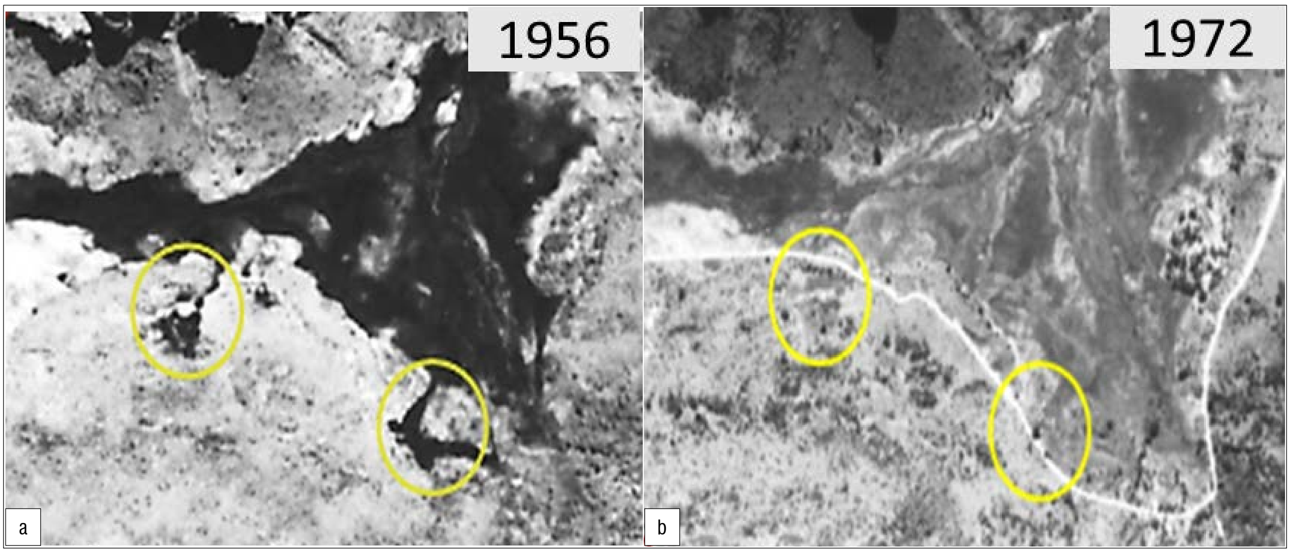

Figure 4: Aerial images of the Matlabas mire taken in (a) 1956 and (b) 1972. The yellow circles show the location of seepage wetlands, which appear to have been significantly reduced after construction of the road, thus indicating changes to the hydrological processes of the mire.

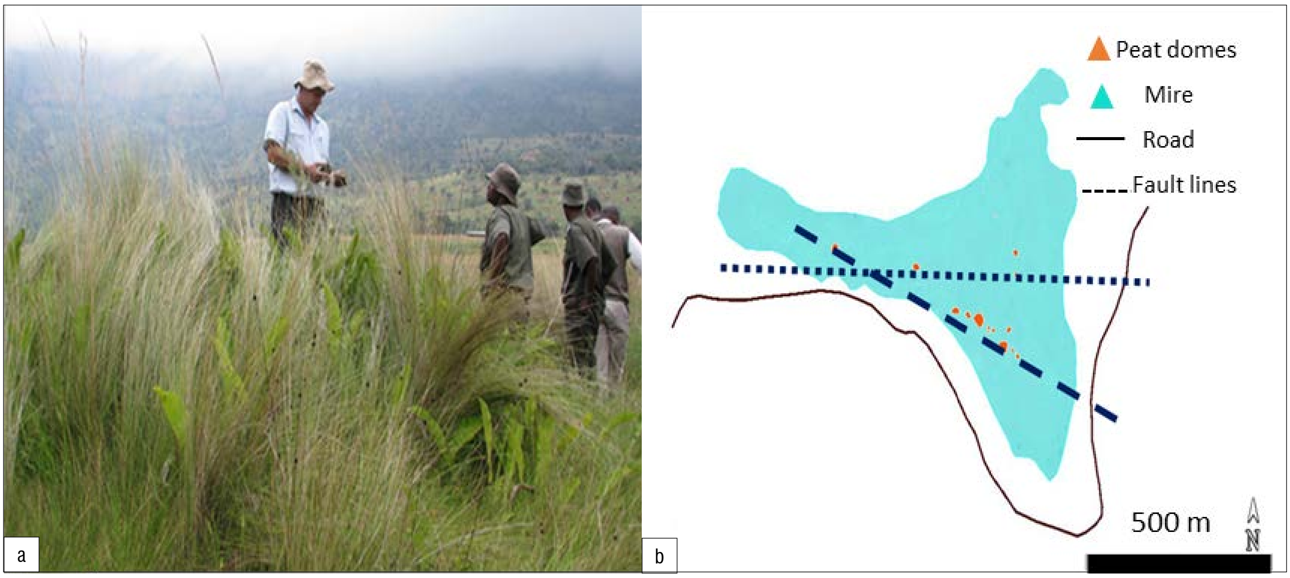

Figure 5: (a) Photograph of one of the small peat domes. (b) Peat dome occurrences and their alignment: NW-SE direction along a previously identified fault line (dashed line) and E-W direction that might indicate another fault line (dotted line).

Vegetation description

From the TWINSPAN analysis, three major plant communities were identified (Figure 6). The three major communities are briefly described below:

1. *Andropogon eucomis–Aristida canescens* community. Most of the elevated peat domes were covered with this vegetation community. This vegetation community contained the largest number of species, with common wetland species as well as species generally associated with drier conditions.
2. *Kyllinga melanosperma–Miscanthus junceus* community. This community occurred in the wettest part of the mire and was closely associated with peat deposits. A stand of *Phragmites australis* reeds on transect B at B3–B4 was found in this vegetation community.
3. *Pteridium aquilinum* community. This community occurred along the edges of the mire and is characterised by species-poor patches dominated by the fern *Pteridium aquilinum*.

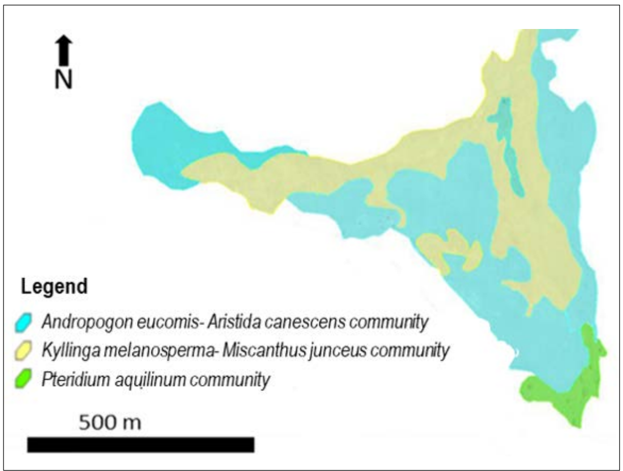

Figure 6: Vegetation map of the mire showing the three dominant vegetation types.

^{14}C dating

Table 1 lists the results of the radiocarbon dating of the 14 peat samples, their δ^{13}C content and descriptions of the depth intervals; the ages are given as median calibrated age. The mire's oldest basal peat sample, with a radiocarbon age of 11 160 CalBP, was taken from point B4f, which is the second lowest point in altitude. The valley flank basal peats all had younger ages, ranging between 5120 CalBP on the southeastern side (AB), 3860 CalBP on the western side (W1) and 690 CalBP on the northeastern side (C3b). Modern dates with bomb values were observed at point B4a (-55 CalBP) and point C3a (-6.5 CalBP), while point B3a dated to 130 CalBP. The δ^{13}C values show that C3 plants were limited to the top layer in core B4 (point B4a), whereas the rest of the samples had values indicating C3 plants.

Groundwater flow

The groundwater phreatic head in the peat layer showed a decrease from east to west along transect B (Figure 7a). At transect C, however, there was a downward direction of the phreatic head isohypse with most of the flow being directed to point C5, which is at the head of a permanent channel. The channel at C5 was shown to be draining from points C4 and C6, which had higher phreatic heads (Figure 7b).

Differences between the piezometric head and the phreatic head were + 0.01 to 0.04 m at B2 and B3, respectively. Such differences indicate potential seepage of groundwater, in line with the depressions visible on the ground surface. The head differences were largest at B4, where differences in the sand piezometric head and peat phreatic head equalled 0.14 m. Similar differences in head were observed along transect C, with the highest piezometric head found under one of the peat domes at point C4. In contrast, the piezometric heads in the sand were lower (c. 0.03 m) than those in the peat further west from B4 and C4 at both transects. At C5, the head difference was also significantly lower at 0.4 m.

Lastly, the water levels in the peat domes were found 30–50 cm below the surface. This depth is different from that of other parts with no dome structures, where the water levels were close to the surface. In the south to north direction, the phreatic head decreased northwards following the height gradient of the mire surface and the drainage direction of the surface water channels.

Peat temperature

Peat temperature showed an increase with depth, with the temperature gradients generally following the gradient of the peat surface slope. However, the discharging groundwater at B4 showed input of warmer water about 1.5 m from the surface: >14 °C when the ambient temperature was 10 °C (Figure 8). These measurements were taken at night during the dry and cold season in August 2013. Such patterns were also found along transects A and C, where warmer temperatures appear to be associated with discharging groundwater flows.

Table 1: Results of ^{14}C dating of the peat samples taken from transects A, B, C on the eastern side and point W1 on the western side

Code	Sample depth (cm)	Altitude (m a.m.s.l)	Sample description and Von Post scale (H1–H10)	δ^{13}C (‰)	Median age (CalBP)	Thickness (m)	Accumulation rate (mm/year)
W1	200	1590.4	Peat with gradual increase of clay content with increasing depth in the 50-cm core, low water content	-12.22	3860	–	–
AB1	250	1584.65	Decomposed peat (H8)	-13.26	5120	–	–
B3a	37	1579.7	Decomposed peat (H6)	-11.62	130	1.00	1.56
B3b	136	1578.03	Peat with high clay content (>H6)	-10.33	590	0.72	0.61
B3c	208	1577.31		-11.43	1780	–	–
B4a	35	1577.63	Red amorphous peat (H1–H3)	-25.88	-55	0.46	1.31
B4b	79	1577.17	Recomposed peat (H6)	-12.29	295	1.42	1.76
B4c	227	1575.75	Radicel peat (H1–H3)	-13.31	1100	0.62	0.66
B4d	282	1575.13	Radicel peat (H1–H3)	-14.46	2040	1.18	1.37
B4e	399	1573.95	Peat with clay and sand interval at 415–425 (>H6)	-15.92	2900	1.00	0.12
B4f	499	1574.95		-13.97	11 160	–	–
B5	155	1575.31	Peat with high clay content (>H6)	-11.53	1225	–	–
C3a	80	1575.52	Decomposed peat (H6)	-10.07	-6.5	1.15	1.65
C3b	195	1574.37	Peat with high clay content (<H6)	-12.96	690	–	–

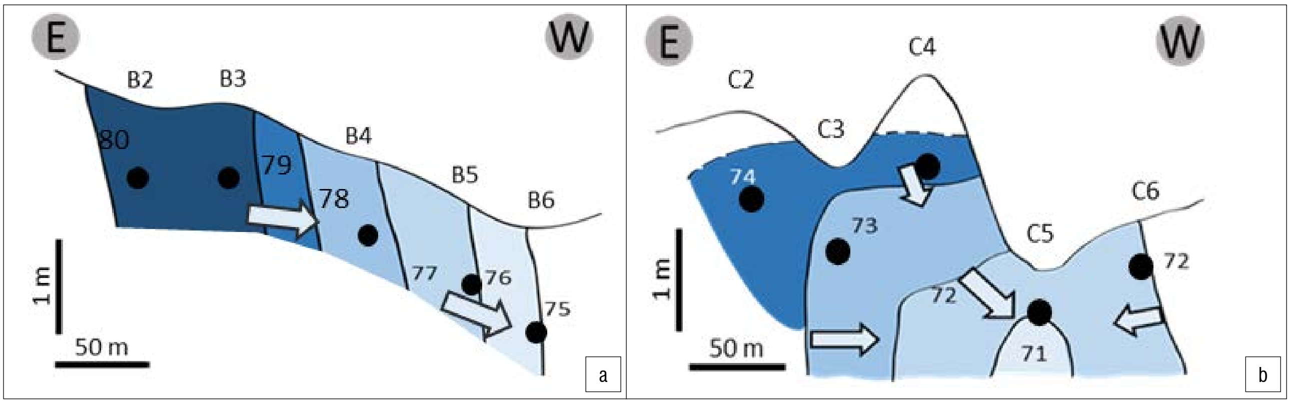

Figure 7: Groundwater phreatic head isohypse in March 2012 along (a) transect B and (b) transect C.

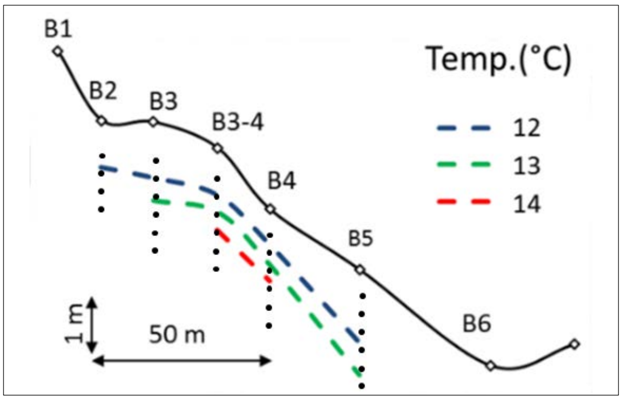

Figure 8: Peat temperature patterns along transect B measured in August 2013.

Ion composition

Chloride ion concentrations changed by three- to fourfold with season in the top 1–2 m of the peat layer. In deeper layers, the changes in concentration were smaller and less than onefold, e.g. at the sand piezometer at B4 (Figure 9a to c). Calcium ion concentrations also increased in the dry seasons, with magnitudes of change similar to patterns in the chloride ion. Calcium values increased by more than threefold within the top 2 m, while it remained one- to twofold higher in the deeper parts, except for B6 which showed higher calcium values in the deeper layers (Figure 9d to f).

In transect C, the calcium-rich and chloride-poor groundwater remained in the deeper soil layers. In the central peat dome, relatively large changes in ion composition occurred. During the wet season the calcium values were low under the peat dome (point C4), while in the dry season the calcium values were higher. There was also an increase in nitrate concentrations (0.73 mg/L relative to the average of 0.16 mg/L) in the

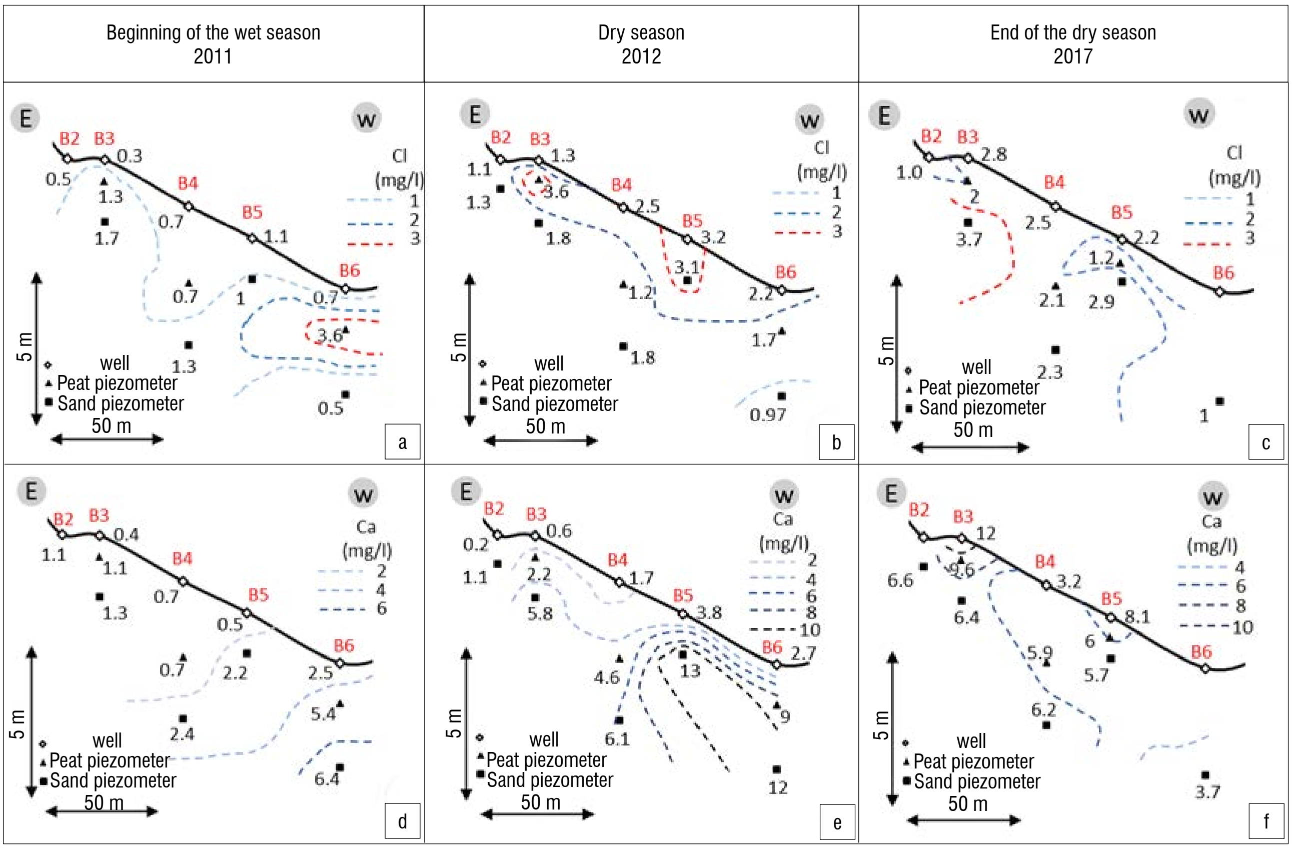

Figure 9: Ion tracers in transect B: (a) chloride at the beginning of the wet season in October 2011, (b) chloride during the dry season in June 2012, (c) chloride at the end of the dry season in October 2017, (d) calcium at the beginning of the wet season in October 2011, (e) calcium during the dry season in June 2012, and (f) calcium at the end of the dry season in October 2017.

groundwater below the peat domes at points C2 and C4 during the wet season (Supplementary table 1).

Stable isotopes

The stable isotope content in the water sampled in March 2015, which was at the end of the hot summer season, was significantly enriched compared with that of the water sampled in October 2017, which was at the end of the cold winter season (Figure 10). The samples from March 2015 had $\delta^{18}O$ values ranging from -4 to -6‰ and $\delta^{2}H$ values ranging from -20 to -30‰, while the samples from October 2017 had $\delta^{18}O$ values ranging from -4 to -3‰ and $\delta^{2}H$ ranging from -10 to -20‰. Samples from the western side of the mire appear to be mostly below the global meteoric water line, with more indications of enrichment.

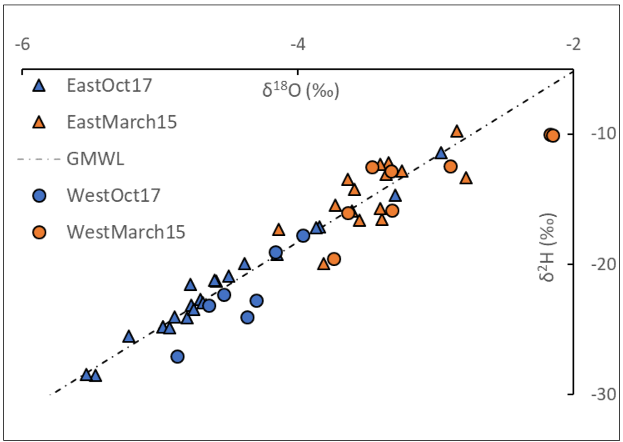

Figure 10: Stable isotope content in water samples from Matlabas. There were 22 water samples taken in March 2015 and 29 water samples taken in October 2017. These samples are labelled according to the side of the mire from which they were sampled: west samples and east samples.

Carbon isotopes

Table 2 shows that four water samples (A2b, B6b, D4b and W5b) had uncorrected ^{14}C values above 100%, indicating infiltration after 1950 and short residence times. Their $\delta^{13}C$ values differed 0 to -15‰. Two samples (B4b and D5b) had $\delta^{13}C$ values around -13‰ and ^{14}C values between 95% and 100%, which indicate infiltration before 1950 and longer residence times.

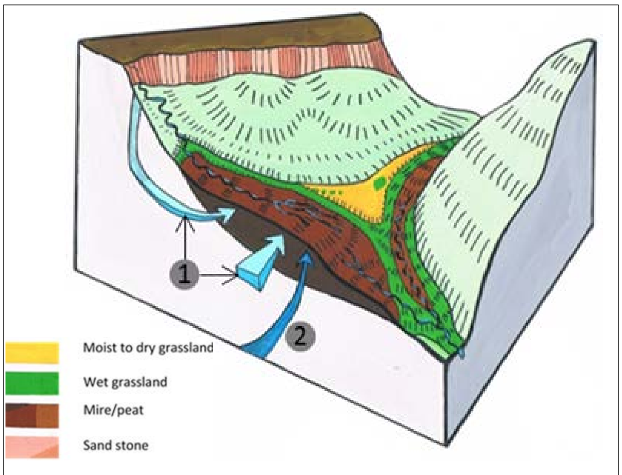

Figure 11: An illustration of the major water flows. 1) Near surface flows: 1a) lateral sheet and phreatic groundwater flow from the hillslopes and 1b) sheet flow above the peat surface during the wet season and 2) deep groundwater flow with a continuous discharge, especially dominant in the dry season.

Table 2: Radiocarbon dating content in six groundwater samples from Matlabas. The samples were taken in October 2017.

No.	Code	Lab no. (GrM)	^{14}C uncorrected (%)	Error ±	$\delta^{13}C$ (‰; IRMS)	Error ±
1	A2b	11547	104.26	0.19	-14.27	0.15
2	B4b	11548	96.42	0.18	-13.38	0.15
3	B6b	11549	104.91	0.19	-10.10	0.15
4	D4b	11550	106.3	0.19	0.43	0.15
5	D5b	11552	95.31	0.18	-13.06	0.15
6	w5b	11554	105.25	0.18	-6.31	0.15

IRMS, isotope ratio mass spectrometry

Discussion

Mire development

Based on radiocarbon dating, peat accumulation began at the lowest parts of the valley on the central eastern side during the transition from the Late Pleistocene to the Holocene. This onset was observed in the thickest peat core obtained at Matlabas, a 5-m peat layer underlain by sand and clay, which was sampled from point B4. Peat accumulation started directly over the mineral soil by paludification processes.[33] The observed sand/clay layers indicate high energy flows during the Early to Mid-Holocene, coupled with an apparently slow peat accumulation rate in the first metre of peat. This accumulation rate indicates initially unstable conditions for accumulating peat.

By the Mid-Holocene, lateral expansion of peat formation had occurred in the higher parts of the valley bottom in the south and west, possibly as a result of a mixture of both autogenic and allogenic factors.[34] Autogenic factors include the clogging effects of peat accumulation on the slope of transect B, with a low hydraulic conductivity leading to a higher water table upslope at transect A in the south and point W1 in the west. With respect to allogenic factors, expansion to the north occurred because of the shift to a wetter climate during the Late Holocene.[34]

In the current vegetation, the wettest vegetation type, which possibly contributes to peat formation, is dominated by the large tussock species *Miscanthus junceus* and also includes stands of *Phragmites australis* at B3 to B4, although *Kyllinga melanosperma* and *Thelypteris confluens* are also abundant. However, the plant remnants in the peat cores were dominated by $\delta^{13}C$ values of C4 plants, which indicates lower water availability.[22,23,35] However, the recent vegetation shows shifts to C3 plants in the best developed and wettest parts of the mire (B4). This modern shift in $\delta^{13}C$ values highlights the role that stable discharge of groundwater flow coupled with the maturity of the peat development plays in sustaining wetter conditions in the mature parts of the mire.

Natural dynamics: water origin and flow

Piezometric head data indicate that groundwater discharge is limited to the central eastern parts of the mire, e.g. at B2 to B4 and C2 to C4. Three major water flows were shown to control mire development (Figure 11).

The first water flow is sheet flow over the peat surface that occurs in the wet season when precipitation exceeds peat infiltration capacity and the peat is often already saturated. The second is the phreatic groundwater flow in the peat layer, which is often also supplied by the intermittent channel in the south that flows in the mire during the wet season with relatively high energy flows, i.e. sand deposits in the soil profiles at transects A and B. The third is the seepage discharge of deeper groundwater at certain points in the mire, e.g. B4 and C4, which is stable and shows little change over the seasons.

The ion composition indicates that the groundwater in Matlabas is generally poor in dissolved minerals, similar to the precipitation water in the Limpopo region.[36] Infiltrating water that passes through the colluvium layer at the valley slopes hardly dissolves any minerals. Hence, the water flows have low concentrations of calcium and mostly depleted stable isotopes, especially during the wet season when the occurrence of rainwater lenses in the top peat layers increases.[37] After a dry period, higher mineral concentrations are evident as a result of concentration by evapotranspiration, particularly in the top layers.

The effects of evaporation could also be observed in the stable isotope values. The variations at the end of the wet period were minor, indicating the stable upward flow of groundwater that is not affected by evaporation. This was, however, not the case for the water flows in the western side of the mire, which has lower hydraulic conductivity in its peat layer. Hence, signs of evaporation were observed in the samples taken from its middle parts during both the hot-wet periods and the cold-dry periods, where the hillslope water enters from the sides, showing a slower flow subject to evaporation processes,[38] and follows the relief to the east side of the mire.

The observed discharges of deep groundwater flow generally had short residence times; however, they had longer flow lines and deeper origins than the phreatic ones. This deeper flow origin is indicated by the radiocarbon values of the water samples. Hence, the sources of these deep discharging groundwater flows are most likely the adjacent hillslopes, which consist of unsorted rock boulders and coarse fragments that form highly permeable layers acting as recharge areas for subsurface water flow to the mire. The groundwater discharges are diluted in the wet period by input from the phreatic and sheet flows, resulting in low calcium and chloride concentrations. However, their chemical characteristics are more nuanced in the dry period with their calcium and bicarbonate-rich groundwater moving vertically upwards, especially at point B4. This deeper groundwater differs distinctly from the shallow groundwater, and their dynamic interactions are most likely to control the vegetation zones, e.g. the *Phragmites australis* reed zone.[39]

Mire features

Geological structures and vegetation also play an important factor in regulating and maintaining the sheet flow during the wet season. The geological fault lines appear to be linked with an upward flow of groundwater, in that the alignment of the peat domes in the northwest-southeast direction resemble the position of a fault line indicated on the 1:250.000 Geological Map.[17] There is also another alignment of peat domes in an east-west direction, which could point to the presence of another fault line.

The large tussocks of the grass *Miscanthus junceus* and the thick rhizomes of the sedge and fern species appear to prevent soil erosion during storm flood events caused by the intermittent stream from the south. The large tussocks are elevated above the water surface, in some instances by as much as 50 cm. They probably reduce the flow velocity and prevent further erosion during storm flood events, with the tussocks and rhizomes dispersing surface water flow so that it does not directly flow into adjacent erosion channels. The vegetation, therefore, is exhibiting a self-organisation mechanism, providing a local positive feedback to stabilise soil against erosion processes.[40]

Anthropogenic disturbance

There are signs of desiccation and release of nutrients, e.g. nitrate concentrations in the dry season, especially in nearby peat dome areas. The desiccation seems to be related to the head cuts in the peat, e.g. at C5. The head cuts not only drain the peat but also expose soil layers to oxidation and infiltration of precipitation water, thus stimulating the presence of acid components in the soil.[41,42] The water pressure data indicate that some desiccated peat domes within the mire, one of which is burnt, have become infiltration areas that lose groundwater to the stream. Also, calcium concentrations in the groundwater below some of the drained peat domes increase significantly during dry periods. The grass *Andropogon eucomis* is a 'moisture-loving' grass. *Aristida canescens* is a hardy grass that grows in poor shallow soil, normally in degraded areas. The presence of this species on the domes can most probably be attributed to the fact that there is a variation in soil moisture on the elevated peat domes which is not suitable for all moisture-loving plant species, hence this grass has established on these elevated areas. We have noted this grass in similar areas in South Africa. It needs to be noted that there are a number of other moisture-loving species that are described in more detail in Bootsma[17]. We connected the peat domes to the fault lines, indicating that these domes have been formed by the deep groundwater exfiltration. The formation of the head-cut channels has led to draining of the mire from its water flows, not limited to the deep groundwater flow, leading to less moisture in the high areas, e.g. the domes and the elevated western side.

The desiccation can be attributed to the change in the land-use practices that have intercepted the sheet flow and the phreatic water supply during the wet seasons. The land-use role in intercepting the natural water flows is also evident from the data available from the unaffected parts of the mire, which reflect stable conditions of groundwater discharge and wetness. The constructed road is a major factor in intercepting the sheet flow at the valley flanks, which is also evident in the disappearance of the seepage wetlands in the south that have now been replaced with non-wetland plant species. The interception of the natural water flow entering the mire has taken place as the road has decreased the space of the flat area separating the hills from the mire, in addition to increased surface run-off via culverts. Another factor responsible for the head cuts is past grazing practices and the current increase in the local elephant population. The vegetation was often burnt in winter to encourage grazing, thereby leading to poor vegetation growth and higher run-off because of reduced vegetation interception of storm flows. Currently, these two factors may be coupled with the appearance of elephant walking paths towards the wet peat areas, where they make bathing pools, which is because of the increasing numbers of elephants since the area became a national park. These paths may lead to accelerated flow, resulting in the initiation of more head cuts. However, these processes require further investigation.

Conclusion

The Matlabas mire started accumulating peat during the Early Holocene; however, the accumulation rate remained very low (0.011 mm/year) until the Mid-Holocene. The maturity of peatland development drives a positive feedback on sustaining wetter conditions for higher accumulation rates. Water availability for plants seems to have shifted to more positive conditions for wetland species in the present, especially in the oldest part of the mire at transect B. Three major water flows were found to support functioning of the mire, namely phreatic groundwater combined with intermittent sheet flow and discharges of locally permanent deep groundwater. The first type of flow had higher water quality during the wet season, when ion composition was diluted by the sheet flow originating from the intermittent channel in the southeast of the mire. During the dry season, this phreatic flow increased in ion concentrations as a result of evaporation processes. The deep groundwater flow was dominant during the dry period, and areas with this type of discharge had more or less stable ion composition throughout the year, e.g. at B4. Land-use practices have had an effect on the less mature parts of the mire by intercepting water from the intermittent channel in the south through the constructed road and formation of head cuts in areas of the mire with grazing and walking paths for cattle and elephants.

Acknowledgements

We acknowledge the staff at SanParks for arranging access and assistance in the park, and the Ecological Restoration Advice (the Netherlands) and the South African Water Research Commission (Project K5/2346) for partial funding. We also thank Althea Grundling and the Agricultural Research Council for helping with the ion composition analysis of the water samples. We also thank the Centre for Isotope Research and the following collaborating colleagues: Harro Meijer, Sanne Palstra and all the Centre staff. Lastly, we thank the staff at the Isotope Environmental Laboratory of iThemba LABS for analysing the stable isotopes in the water.

Authors' contributions

A.B.: Research design; fieldwork; writing. S.E.: Research design; fieldwork; laboratory analysis; writing. A.G.: Research design; fieldwork; student supervision; writing. P-L.G.: Research design; fieldwork; student supervision; writing. S.K.: Research design; fieldwork; writing. M.B.: Laboratory analysis; writing. L.B.: Research design; fieldwork; student supervision; writing. P.S.: Research design; fieldwork; student supervision; writing.

References

1. Clymo RS, Turunen J, Tolonen K. Carbon accumulation in peatland. Oikos. 1998;81(2):368–388. http://dx.doi.org/10.2307/3547057
2. Joosten H, Clarke D. Wise use of mires and peatlands. Greifswald, Germany: International Mire Conservation Group and International Peat Society. 2002; p. 304.
3. Mitsch WJ, Gosselink JG. The value of wetlands: Importance of scale and landscape setting. Ecol Econ. 2000;35(1):25–33. http://dx.doi.org/10.1016/s0921-8009(00)00165-8
4. Bonn A, Allott T, Evans M, Joosten H, Stoneman R. Peatland restoration and ecosystem services: An introduction. In: Bonn A, Allott T, Evans M, Joosten H, Stoneman R, editors. Peatland restoration and ecosystem services. Cambridge, UK: Cambridge University Press; 2016. p. 1–16. https://doi.org/10.1017/CBO9781139177788
5. Joosten H, Tanneberger F, Moen A, editors. Mires and peatlands of Europe: Status, distribution and conservation. Stuttgart: Schweizerbart Science; 2017.
6. Yu Z, Loisel J, Brosseau DP, Beilman DW, Hunt SJ. Global peatland dynamics since the Last Glacial Maximum. Geophys Res Lett. 2010;37(13), L13402, 5 pages. http://dx.doi.org/10.1029/2010gl043584
7. Grundling PL, Grobler R. Peatlands and mires of South Africa. Stapfia. 2005;85:379–396.
8. Thamm AG, Grundling P, Mazus H. Holocene and recent peat growth rates on the Zululand coastal plain. J Afr Earth Sci. 1996;23(1):119–124. http://dx.doi.org/10.1016/s0899-5362(96)00056-5
9. Meadows ME. The role of Quaternary environmental change in the evolution of landscapes: Case studies from southern Africa. CATENA. 2001;42(1):39–57. http://dx.doi.org/10.1016/s0341-8162(00)00115-6
10. Meijer HAJ. Stable isotope quality assurance using the "Calibrated IRMS" strategy. Isotopes Environ Health Stud. 2009;45(2):150–163. http://dx.doi.org/10.1080/10256010902869113
11. Grundling P, Grootjans AP, Price JS, Ellery WN. Development and persistence of an African mire: How the oldest South African fen has survived in a marginal climate. CATENA. 2013;110:176–183. http://dx.doi.org/10.1016/j.catena.2013.06.004
12. Baker A, Routh J, Blaauw M, Roychoudhury AN. Geochemical records of palaeoenvironmental controls on peat forming processes in the Mfabeni peatland, Kwazulu Natal, South Africa since the Late Pleistocene. Palaeogeogr Palaeoclim Palaeoecol. 2014;395:95–106. http://dx.doi.org/10.1016/j.palaeo.2013.12.019
13. Grundling P, Grundling AT, Pretorius L, Mulders J, Mitchell S. South African peatlands: ecohydrological characteristics and socio-economic value. WRC report no. 2346/1/17. Pretoria: Water Research Commission; 2017.
14. Trambauer P, Maskey S, Werner M, Pappenberger F, Van Beek LPH, Uhlenbrook S. Identification and simulation of space–time variability of past hydrological drought events in the Limpopo River basin, southern Africa. Hydrol Earth Syst Sci. 2014;18(8):2925–2942. http://dx.doi.org/10.5194/hess-18-2925-2014
15. SanParks. Marakele National Park: Park Management Plan for the period 2014–2024 [document on the Internet]. c2014 [cited 2017 Mar 20]. Available from: https://www.sanparks.org/assets/docs/conservation/park_man/marakele_approved_plans.pdf
16. Van Staden PJ. An ecological study of the plant communities of Marakele National Park [MSc thesis]. Pretoria: University of Pretoria; 2002.
17. Bootsma A. Mechanisms of erosion prevention and stabilization in a Marakele peatland; implications for conservation management [MSc thesis]. Pretoria: University of South Africa; 2016.
18. South African Committee for Stratigraphy (SACS). Kent LE, compiler. Stratigraphy of South Africa handbook 8. Part 1: Lithostratigraphy of the Republic of South Africa, South West Africa/ Namibië and the Republics of Bophuthatswana, Transkei, and Venda. Pretoria: Government Printer; 1980.
19. Westhoff V, Van Der Maarel E. The Braun-Blanquet approach. In: Whittaker RH, editor. Classification of plant communities. The Hague: Springer; 1978. p. 287–399. http://dx.doi.org/10.1007/978-94-009-9183-5_9
20. Brown LR, Du Preez PJ, Bezuidenhout H, Bredenkamp GJ, Mostert THC, Collins NB. Guidelines for phytosociological classifications and descriptions of vegetation in southern Africa. Koedoe. 2013;55(1), Art. #1103, 10 pages. http://dx.doi.org/10.4102/koedoe.v55i1.1103
21. Peet RK, Roberts DW. Classification of natural and semi-natural vegetation. In: Van der Maarel E, Franklin J, editors. Vegetation ecology. 2nd ed. Chichester: John Wiley & Sons; 2013. p. 28–70. http://dx.doi.org/10.1002/9781118452592.ch2
22. Roleček J, Tichý L, Zelený D, Chytrý M. Modified TWINSPAN classification in which the hierarchy respects cluster heterogeneity. J Veg Sci. 2009;20(4):596–602. http://dx.doi.org/10.1111/j.1654-1103.2009.01062.x
23. O'Leary MH. Carbon isotope fractionation in plants. Phytochemistry. 1981;20(4):553–567. http://dx.doi.org/10.1016/0031-9422(81)85134-5
24. O'Leary MH. Carbon isotopes in photosynthesis. BioScience. 1988;38(5):328–336. http://dx.doi.org/10.2307/1310735
25. Von Post L. Sveriges Geologiska Undersöknings torvinven- tering och några av dess hittills vunna resultat [Sweden's geological survey of peat turf and some results so far]. Svenska moss-kulturföreningens tidskrift 37. 1922:1–27. Swedish.
26. Aerts-Bijma AT, Van der Plicht J, Meijer HAJ. Automatic AMS sample combustion and CO_2 collection. Radiocarbon. 2001;43(2A):293–298. http://dx.doi.org/10.1017/s0033822200038133
27. Mook WG, Van der Plicht J. Reporting ^{14}C activities and concentrations. Radiocarbon. 1999;41(03):227–239. http://dx.doi.org/10.1017/s0033822200057106
28. Ramsey CB. Deposition models for chronological records. Quat Sci Rev. 2008;27(1–2):42–60. http://dx.doi.org/10.1016/j.quascirev.2007.01.019
29. Hogg AG, Hua Q, Blackwell PG, Niu M, Buck CE, Guilderson TP, et al. SHCal13 Southern hemisphere calibration, 0–50,000 years cal BP. Radiocarbon. 2013;55(04):1889–1903. http://dx.doi.org/10.2458/azu_js_rc.55.16783
30. Hua Q, Barbetti M, Rakowski AZ. Atmospheric radiocarbon for the period 1950–2010. Radiocarbon. 2013;55(04):2059–2072. http://dx.doi.org/10.2458/azu_js_rc.v55i2.16177
31. Van Wirdum, G. Vegetation and hydrology of floating ricsh fens [PhD thesis]. Amsterdam: University of Amsterdam; 1991.
32. Mook WG. Introduction to isotope hydrology: Stable and radioactive isotopes of hydrogen, oxygen and carbon. London: Taylor & Francis; 2006.
33. Charman D. Peatlands and environmental change. Chichester: John Wiley & Sons; 2002.
34. Anderson RL, Foster DR, Motzkin G. Integrating lateral expansion into models of peatland development in temperate New England. J Ecol. 2003;91(1):68–76. http://dx.doi.org/10.1046/j.1365-2745.2003.00740.x
35. Scott L. Evidence for environmental conditions during the last 20000 years in southern Africa from ^{13}C in fossil hyrax dung. Glob Planet Change. 2000;26(1–3):207–215. http://dx.doi.org/10.1016/s0921-8181(00)00045-x
36. Van Wyk E, Van Tonder G, Vermeulen D. Characteristics of local groundwater recharge cycles in South African semi-arid hard rock terrains – rainwater input. Water SA. 2011;37(2):147–154. http://dx.doi.org/10.4314/wsa.v37i2.65860
37. Schot P, Dekker S, Poot A. The dynamic form of rainwater lenses in drained fens. J Hydrol. 2004;293(1–4):74–84. http://dx.doi.org/10.1016/j.jhydrol.2004.01.009
38. Gat JR. Oxygen and hydrogen isotopes in the hydrologic cycle. Annu Rev Earth Planet Sci. 1996;24(1):225–262. http://dx.doi.org/10.1146/annurev.earth.24.1.225
39. De Mars H, Wassen MJ, Venterink HO. Flooding and groundwater dynamics in fens in eastern Poland. J Veg Sci. 1997;8(3):319–328. http://dx.doi.org/10.1111/j.1654-1103.1997.tb02628.x
40. Eppinga MB, Rietkerk M, Wassen MJ, De Ruiter PC. Linking habitat modification to catastrophic shifts and vegetation patterns in bogs. Plant Ecol. 2007;200(1):53–68. http://dx.doi.org/10.1007/s11258-007-9309-6
41. Brady N, Weil R. Nature and properties of soils. 12th ed. Upper Saddle River, NJ: Prentice Hall; 1998.
42. Madaras M, Grootjans AP, Šefferová Stanová V, Janáková M, Laštůvka Z, Jansen A. Fen meadows of Abrod; in urgent need of protection. In: Grootjans AP, Jansen AMJ, Stanova V, editors. Calcareous mires of Slovakia; landscape setting, management and restoration prospects. Leiden: Brill; 2012. p. 77–96. http://dx.doi.org/10.1163/9789004277960_008